Environ Monit Assess (2021) 193: 642
https://doi.org/10.1007/s10661-021-09389-0

Preparation of melon peel biochar/$CoFe_2O_4$ as a new adsorbent for the separation and preconcentration of Cu(II), Cd(II), and Pb(II) ions by solid-phase extraction in water and vegetable samples

Duygu Ozdes · Celal Duran

Received: 2 March 2021 / Accepted: 10 August 2021

Abstract The present research describes the successful preparation of melon peel biochar modified with $CoFe_2O_4$ (MPBC/$CoFe_2O_4$) followed by its usage as a new sorbent to separate, preconcentrate, and determine the toxic heavy metal ions by magnetic solid-phase extraction. The metal ion desorption was performed by 0.1 M HCl solution with a volume of 5.0 mL. Flame atomic absorption spectrometry (FAAS) was utilized for detection of the analyte levels. SEM–EDX, TEM, XRD, and FTIR techniques were carried out to illuminate the structure of MPBC/$CoFe_2O_4$. The fundamental variables affecting the adsorption and elution efficiencies of the analyte ions including solution pH, MPBC/$CoFe_2O_4$ amount, type and concentration of eluent, adsorption and desorption equilibrium time, and sample volume were optimized. The detection limits were calculated as 0.41, 1.82, and 3.16 μg L^{-1} for Cu^{2+}, Cd^{2+}, and Pb^{2+} ions, respectively, with the relative standard deviation of lower than 4.2%. There were no substantial interference effects on the analyte ion recovery due to the presence of foreign ions at high levels. Five minutes of contact time was adequate to attain the adsorption equilibrium. The adsorption capacity of MPBC/$CoFe_2O_4$ was obtained as 106.4, 65.4, and 188.7 mg g^{-1} for Cu^{2+}, Cd^{2+}, and Pb^{2+} ions, respectively, by utilizing Langmuir isotherm model. The pseudo-second order model is favorable to identify the adsorption kinetics. The method was validated by spike/recovery test, and then, it was successfully implemented to determine the aforementioned analyte levels in sea and stream water, pepper, black cabbage, eggplant, and tomato samples.

Keywords Cadmium · Copper · Lead · Melon peel biochar/$CoFe_2O_4$ · Preconcentration · Separation · Solid-phase extraction

Introduction

The inevitable increment in the concentration of persistent trace heavy metals in the environment through a variety of industrial, agricultural, and technological activities has attracted more attention in recent years by virtue of their detrimental impacts on living organisms. Lead and cadmium ions are among heavy metals that have extremely toxic effects even at very low concentrations since they induce inhibition or even deprivation of the biological functions of enzymes in living organisms and ultimately cause incredibly negative damages to the nervous, reproductive, and circulatory

---

D. Ozdes
Gumushane Vocational School, Chemistry and Chemical Processing Technologies Department, Gumushane University, 29100 Gumushane, Turkey

C. Duran (✉)
Faculty of Sciences, Department of Chemistry, Karadeniz Technical University, 61080 Trabzon, Turkey
e-mail: cduran@ktu.edu.tr

systems (Huang et al., 2020; Zhao et al., 2016). Moreover, the accumulation of Cd^{2+} and Pb^{2+} ions in human body may impair the brain functions and provoke cancer diseases. Although copper is a requisite trace metal for humans, animals, and plants in certain concentrations since it acted as a cofactor in enzymatic reactions, it causes various diseases including cramps, spasms, vomiting, or even death if taken in excess amounts (Dahaghin et al., 2017; Tu et al., 2016). The maximum allowable Cu^{2+}, Cd^{2+}, and Pb^{2+} ions levels designated by the World Health Organization (WHO)-Food and Agriculture Organization (FAO) in vegetables are 73.0, 0.10, and 0.30 mg kg^{-1}, respectively, while the tolerable levels of these ions in drinking water recommended by WHO are 2.0, 0.01, and 0.003 mg L^{-1}, respectively (Behbahani et al., 2013; Bigdeli & Seilsepour, 2008). Therefore, the precise determination and monitoring of the toxic metal ions contents both in water and food samples are surpassingly important task for scientist.

Numerous analytical techniques including UV–Visible spectrometry, inductively coupled plasma-mass spectrometry, electroanalytical methods, and flame or graphite furnace atomic absorption spectrometry have been employed in the routine detection of trace heavy metal levels. The complicated matrix that consists of a great number of concomitant cations and anions together with heavy metal ions to be analyzed and the lower concentrations of heavy metals than the quantification limit of the aforementioned instrumental techniques restrict the accurate and sensitive analysis (Gouda, 2014). To come through these troubles, a convenient separation and preconcentration method including solid-phase extraction (Yağci et al., 2020), coprecipitation (Tufekci et al., 2013), liquid–liquid extraction (Farajvand et al., 2019), membrane filtration (Soylak et al., 2004), and cloud point extraction (Rahnama & Najafi, 2016) is generally employed prior to analysis.

Solid-phase extraction (SPE) is regarded as a versatile and efficient method with respect to its simplicity and rapidity, usage of less organic solvents in the process, enabling the development of a wide variety of low cost and effective adsorbents, and achieving the high preconcentration factors that allows detecting the extremely low levels of metal ions in the environmental real samples (Tokay & Bagdat, 2019). Besides, the magnetic solid-phase extraction (MSPE) is useful types of SPE method since it enables to separate the utilized adsorbent from high volume of solutions by applying a magnet instead of time consuming filtration or centrifugation. The properties of the selected adsorbents significantly affect the performance of the SPE method (Kanani et al., 2018).

Biochar is a type of carbon-rich substance fabricated by thermal decomposition of organic materials such as apple pomace (Zhang et al., 2019), dew melon peel (Ahmadi et al., 2016), pine bark (Reddy & Lee, 2014), banana and orange peels (Amin et al., 2019), and potato leaves (Zhao et al., 2019) under limited oxygen conditions and at a temperature in the range of 200–900 °C. The utilization of biochar produced from fruit peels has attracted attention due to its abundance and cheapness. Biochar, which is an eco-friendly and cost-effective adsorbent, has a large specific surface area and porous structure, and there are various functional groups on its structure that allow the adsorption of metal ions (Reddy & Lee, 2014). By the reason of low density and small particle size of the biochars, the collection of them from aqueous solutions is considered as a fundamental problem that limits its large-scale application. The magnetic biochar that has an excellent performance in adsorbing the metal ions can be separated easily utilizing an external magnetic field. It is prepared properly by inducing magnetic particles into biochar (Li et al., 2020; Zhang et al., 2019). Magnetic nanoparticles formulated via MFe_2O_4 have drawn considerable attention as adsorbent due to their magnificent chemical and physical characteristics. In that formula, "M" can be Mn, Zn, Co, Mg, Fe, and Cu atoms (Ramadan, 2019). The cobalt ferrite ($CoFe_2O_4$) is commonly preferred magnetic material due to its chemical and thermal stability, high mechanical hardness, easy preparation and separation, and biodegradability. Kanani et al. (2018) have prepared a new magnetic adsorbent by coating MCM-41 with $CoFe_2O_4$ and piperazine to separate and preconcentrate the Cu^{2+}, Cd^{2+}, and Pb^{2+} ions prior to FAAS analysis. Reddy and Lee (2014) have demonstrated an effortless preparation of magnetic biochar with pine bark and $CoFe_2O_4$ to be utilized as an adsorbent for retention of Pb^{2+} and Cd^{2+} ions from aqueous media. Foroutan et al. (2018) have modified the *Phoenix dactylifera* stones activated carbon with $CoFe_2O_4$ to use as an adsorbent in Cr(VI) uptake.

In the present research, a new and effective magnetic adsorbent, melon peel biochar/$CoFe_2O_4$ (MPBC/$CoFe_2O_4$) nanoparticles, has been synthesized and characterized. The MPBC/$CoFe_2O_4$ has been applied to separate and preconcentrate the Cu^{2+}, Cd^{2+}, and Pb^{2+} ions in water and vegetable samples by MSPE method. The predominant experimental variables affecting the adsorption and desorption yields of the analyte ions have been evaluated and optimized to obtain the satisfactory recovery values. By this work, a sensitive, effective, economical, and eco-friendly separation and preconcentration technique is considered to be developed for the simultaneous determination of heavy metal ions from food and water samples by FAAS.

Materials and methods

Instrumentation

The morphology and elemental composition of MPBC and MPBC/$CoFe_2O_4$ was assessed by the scanning electron microscope with an energy-dispersive X-ray spectrometer (SEM–EDX, ZIESS SIGMA 300). Transmission electron microscope (TEM, Hitachi HT7700) was used to evaluate the microstructure of the adsorbents. The Fourier transform infrared spectrometer (PerkinElmer 1600 FT-IR Spectrophotometer) was utilized to identify the surface functional groups of MPBC and MPBC/$CoFe_2O_4$. The structure of the MPBC/$CoFe_2O_4$ was scrutinized through X-ray diffraction (XRD) measurements (Rigaku TTR III) with Cu Kα radiation ($\lambda = 1.5406$ Å) in the 2Θ range of 5–80°. A PerkinElmer AAnalyst 400 model Flame Atomic Absorption Spectrometer was employed to determine the metal ions levels. The device was equipped with deuterium background system and air/acetylene burner. The wavelengths for Cu^{2+}, Cd^{2+}, and Pb^{2+} ions were selected as 324.75, 228.80, and 283.31 nm, respectively, and other working conditions of the instrument were designated by considering the manufacturer's recommendations. The pH adjustment was carried out by utilizing a Hanna pH-211 digital pH meter. The batch adsorption and desorption experiments were performed by mechanical shaker (Edmund Bühler GmbH). A closed vessel microwave system (Milestone Ethos D) was operated to digest the vegetable samples. Analytical balance (Sartorius BP 1106) and heating magnetic stirrer (IKA RCT Basic) were utilized in the studies when needed.

Reagents

All the chemical reagents used at different stages of the experiments including nitric acid (HNO_3, 65%), sodium hydroxide (NaOH), hydrochloric acid (HCl, 37%), hydrogen peroxide (H_2O_2, 30%), iron(III) chloride hexahydrate ($FeCl_3 \cdot 6H_2O$), and cobalt(II) nitrate hexahydrate ($Co(NO_3)_2 \cdot 6H_2O$) and all the salts employed for the interference study are of analytical grade supplied from Sigma-Aldrich (Shanghai, China) and Merck (Darmstadt, Germany) and used without any additional purification process. To obtain the desired concentration of the standard and working solutions of Cu^{2+}, Cd^{2+}, and Pb^{2+} ions, stock solutions (1000 mg L^{-1}) of these ions prepared in 2% (v/v) HNO_3 solution were diluted with distilled water in the appropriate amounts. The glassware utilized in the experiments was kept overnight in 5% (v/v) HNO_3 and washed thoroughly with tap water and then with distilled water before use.

Preparation of melon peel biochar/$CoFe_2O_4$

The melon was purchased from a greengrocer in Gümüşhane, Turkey, and its peel was collected for the preparation of adsorbent. After washed the melon peels with distilled water, it was cut into small pieces. Then, it was first kept in an open atmosphere for 3 days to remove of moisture and then dried in an oven at 60 °C for 24 h. The sufficient amount of melon peel was put in a porcelain crucible and carbonized in a muffle furnace at 450 °C under oxygen limited conditions. The holding time and heating rate were kept as 60 min and 10 °C/min, respectively. After the resulting melon peel biochar (MPBC) was cooled down to room temperature, it was grinded in an agate mortar and preserved in a plastic container until it was needed (Ahmadi et al., 2016).

The MPBC/$CoFe_2O_4$ was prepared briefly as follows: 5.0 g of MPBC was mixed with 3.66 g of $Co(NO_3)_2 \cdot 6H_2O$ and 6.80 g of $FeCl_3 \cdot 6H_2O$ (molar ratio of $Fe^{3+}/Co^{2+} = 2$) in 200 mL of aqueous solution. In order to provide an opportunity for the penetration of Fe and Co ions into the MPBC pores, the mixture was stirred vigorously for 20 min and increased the temperature to 90 °C. The NaOH solution (3.0 M) was slowly added until the pH of the solution was 10, and the mixture was stirred for 120 min. Thereafter, the MPBC/$CoFe_2O_4$ was collected by filtration, washed thoroughly with distilled water up to neutral pH, and dried in an oven at 105 °C for 24 h (Foroutan et al., 2018; Mehrabi et al., 2017).

Model solutions

The batch technique was carried out to separate and preconcentrate the Cu^{2+}, Cd^{2+}, and Pb^{2+} ions based on SPE method. The general procedure is as follows: 0.10 g of MPBC/$CoFe_2O_4$ (2.0 g L^{-1}) was added to 50 mL of aqueous solution containing 0.4 mg L^{-1} of Pb^{2+}, 0.1 mg L^{-1} of Cd^{2+}, and 0.2 mg L^{-1} of Cu^{2+} ions. Diluted NaOH or HNO_3 solutions were utilized for the adjustment of pH to its optimum value of 5.0. The mixture was shaken on a mechanical shaker at room temperature for 5 min at 400 rpm to achieve the equilibrium. At the end of this period, the metal-loaded MPBC/$CoFe_2O_4$ was accumulated at the bottom of the centrifuge tube with an external magnet and then the supernatant was discarded. Afterwards, the adsorbent was treated with 5.0 mL of 0.1 M HCl solution for 5 min to elute the metal ions. Finally, the MPBC/$CoFe_2O_4$ was magnetically removed from the solution and the levels of the analyte ions were analyzed in the supernatant by FAAS. The factors affecting the adsorption and desorption conditions of the metal ions including pH, contact time, MPBC/$CoFe_2O_4$ quantity, eluent type, concentration and volume, and sample volume were studied in detailed and optimized.

Real sample preparation

The MPBC/$CoFe_2O_4$ was implemented successfully for the detection of the analyte ions in water (sea and stream water) and vegetable (pepper, black cabbage, eggplant, and tomato) samples. The seawater (Blacksea, Trabzon, Turkey) and stream water (Değirmendere, Trabzon, Turkey) were filtered by using cellulose nitrate membrane as soon as they were collected. After the samples were acidified, they were kept at 4 °C in the refrigerator in polyethylene bottles until analysis. For implementation of the method, the pH of the 250 mL of water samples (optimum sample volume) was set to 5.0 and the required amount of MPBC/$CoFe_2O_4$ was added. Then, the presented SPE method was carried out to determine their Cu^{2+}, Cd^{2+}, and Pb^{2+} levels. The vegetable samples were purchased from a greengrocer in Gümüşhane, Turkey. Before digestion, the samples were washed thoroughly with distilled water, dried in an oven at 80 °C for 12 h, and then ground in an agate mortar. The vegetable samples were digested by the closed vessel microwave digestion system. For that purpose, 0.750 g of pepper, black cabbage, eggplant, and tomato samples was weighted into the separate Teflon vessels accurately and digested with 6 mL of HNO_3 and 2 mL of H_2O_2 in microwave system (Duran et al., 2009b).

Results and discussions

Adsorbent characterization

The surface morphology of MPBC and MPBC/$CoFe_2O_4$ was assessed by scanning electron microscopy (SEM) technique. The SEM image of MPBC disclosed its rough and slightly porous structure which is suitable for the aggregation of $CoFe_2O_4$ nanoparticles (Fig. 1a). The SEM image given in Fig. 1b indicated the attachment of $CoFe_2O_4$ on MPBC surface. The EDX spectra of MPBC (Fig. 2a) and MPBC/$CoFe_2O_4$ (Fig. 2b) display their elemental composition. MPBC contains 44.36% of C, 54.76% of O, and 0.88% of Fe. When the content of the MPBC/$CoFe_2O_4$ was evaluated, it is seen that the amount of Fe (26.04%) increases significantly and a Co peak (7.56%) is also formed in the spectrum. The EDX results indicated the presence of $CoFe_2O_4$ on the MPBC surface. Li et al. (2021) observed a similar elemental composition for $CoFe_2O_4$-biochar by using SEM–EDX method. The morphology of the adsorbents was

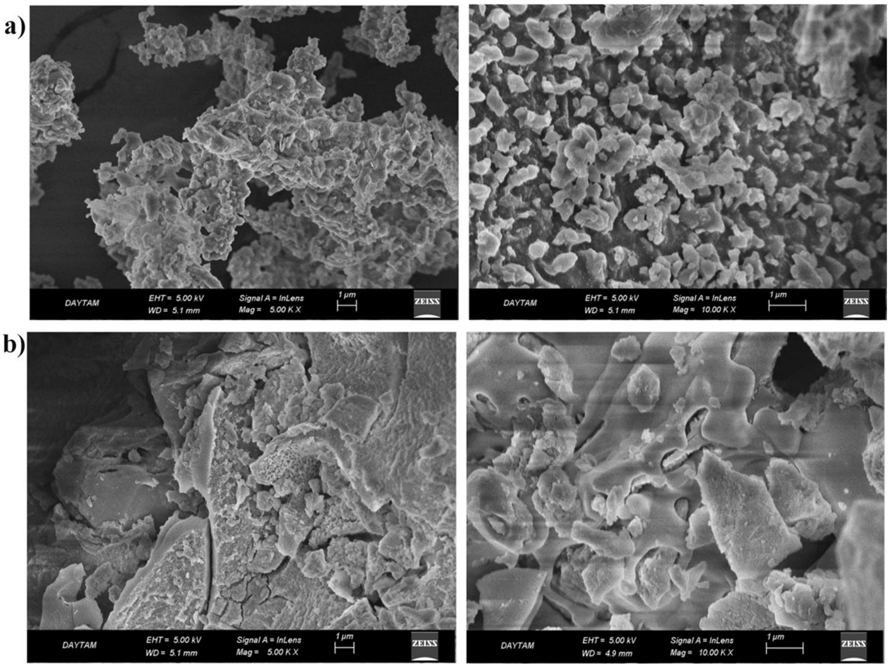

Fig. 1 SEM micrographs of **a** MPBC and **b** MPBC/$CoFe_2O_4$

further evaluated by utilizing TEM. By comparing the TEM images of MPBC (Fig. 3a) and MPBC/$CoFe_2O_4$ (Fig. 3b), it is noticed that $CoFe_2O_4$ nanoparticles were distributed on a regular basis

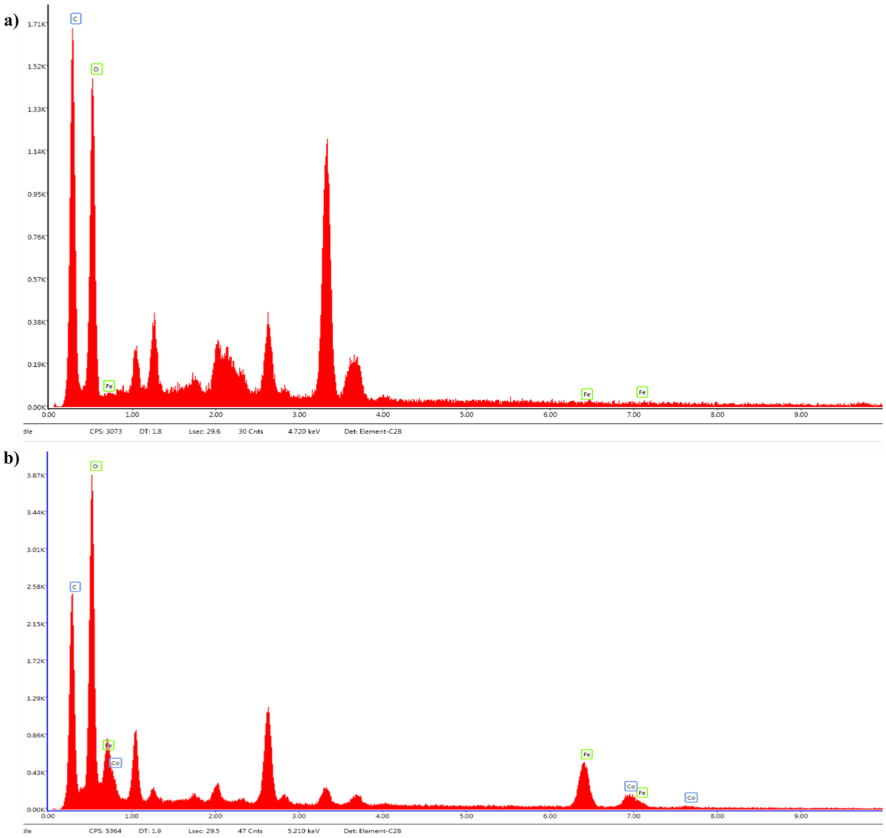

Fig. 2 EDX images of **a** MPBC and **b** MPBC/$CoFe_2O_4$

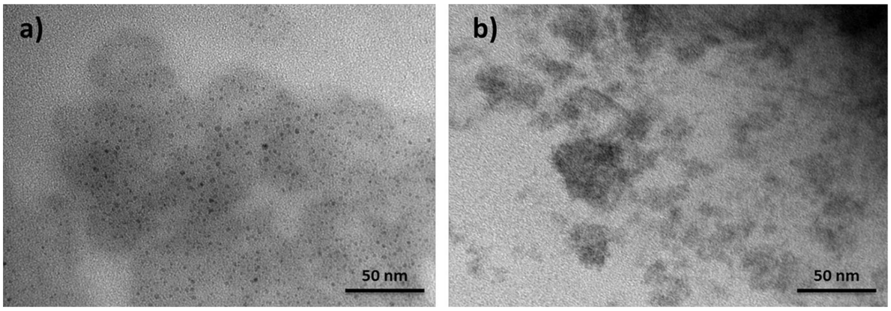

Fig. 3 TEM images of **a** MPBC and **b** MPBC/$CoFe_2O_4$

dramatically in the MPBC matrix. The XRD pattern of MPBC/$CoFe_2O_4$ is shown in Fig. 4. The characteristic peaks (2Θ = 30.2°, 35.5°, 43.2°, and 57.2°) correspond to crystal indexes of 220, 311, 400, and 511 indicating the formation of cubic spinel type lattice of MPBC/$CoFe_2O_4$ (Rahimi et al., 2018). Similar XRD pattern was obtained by You et al. (2021) for the magnetic corn stalks biochar/$CoFe_2O_4$ complex. FTIR spectroscopy was utilized to acquire information about the surface functional groups of the adsorbents. Both MPBC and MPBC/$CoFe_2O_4$ possess several peaks on their structure confirming the presence of polysaccharides and polyphenols. The small peaks at 2926 cm^{-1} and 1460 cm^{-1} were related to aliphatic $-CH_2$ stretching while the peaks at 1390, 1112, 1040, and 700–900 cm^{-1} were attributed to aliphatic –OH, phenolic –OH, C–O, and aromatic C–H species, respectively (Fig. 5a) (Han et al., 2021). By comparing the FTIR spectrum of MPBC and MPBC/$CoFe_2O_4$, it is noticed that some peaks have shifted and several new peaks have formed. A stretching vibration at 3320 cm^{-1} in the FTIR spectra of MPBC/$CoFe_2O_4$ was attributed to O–H bonds. The MPBC/$CoFe_2O_4$ showed a peak at 570 cm^{-1} (Fig. 5b), corresponding to the Fe–O stretching mode of the $CoFe_2O_4$ (Reddy & Lee, 2014; Zhou et al., 2014). When the characterization results are evaluated in general, it can be concluded that the $CoFe_2O_4$ was smoothly loaded onto MPBC.

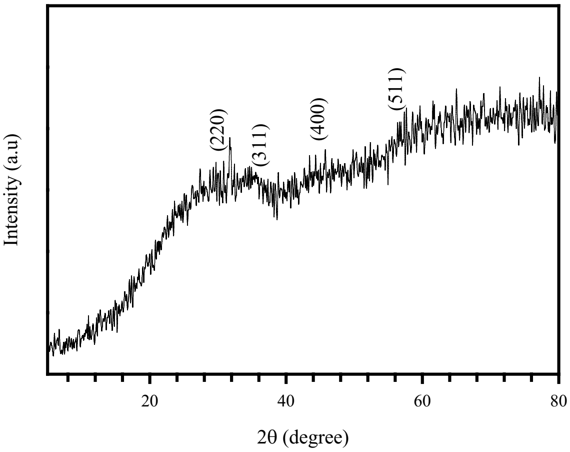

Fig. 4 XRD patterns of MPBC/$CoFe_2O_4$

Effect of pH on the extraction of analyte ions

The pH of aqueous media has a crucial impact with respect to extraction efficiency of the metal ions since the H_3O^+ ion concentration of solution, the ionization degree of the surface functional groups of an adsorbent, and also speciation of the metal cations are directly affected by the medium pH (Khan et al., 2016). Therefore, the influence of pH on the extraction efficiency of Cu^{2+}, Cd^{2+}, and Pb^{2+} ions was scrutinized by varying the solution pH in the range of 2.0–8.0 with keeping other experimental parameters constant. Based on the obtained data, the analyte ions recovery increased sharply when the solution pH increased from 2.0 to 5.0, and then, it remained nearly constant in the pH range of 5.0–8.0 (Fig. 6). The recovery percentages were below than 15% at pH 2.0 and higher than 96% in the pH range of 5.0–8.0 for all analyte ions. At lower pH values, the competition between the H_3O^+ ions and the metal cations to bind to the active adsorption sites on MPBC/$CoFe_2O_4$ surface could be resulted in low recovery values. Furthermore, the protonation of MPBC/$CoFe_2O_4$ surface at highly acidic pH values induces an electrostatic repulsion between the adsorbent surface and the metal cations. Conversely, when the solution

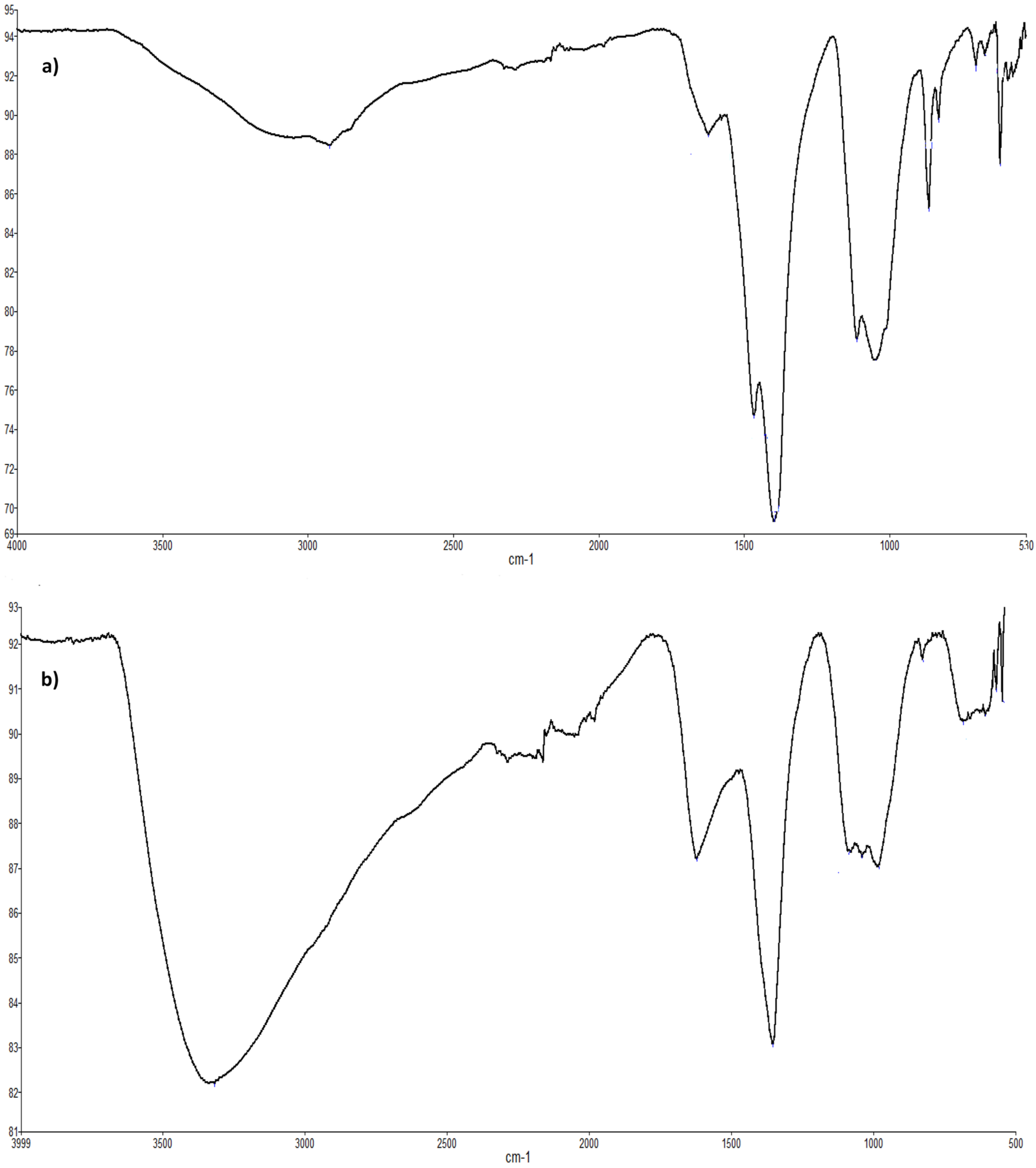

Fig. 5 FTIR spectrum of **a** MPBC and **b** MPBC/$CoFe_2O_4$

pH was increased, the surface charge of MPBC/$CoFe_2O_4$ become more negative because of the presence of excess hydroxide ions, which lead to adsorption of positively charged metal ions substantially (Sun et al., 2015). As a result, the pH 5.0 was specified as optimum pH for the subsequent studies. Suo et al. (2019) also reported that pH 5.0 was the optimum value for simultaneous MSPE of Cr^{3+}, Co^{2+}, Ni^{2+}, Cu^{2+}, Pb^{2+}, Cd^{2+}, and Ag^{+} ions in environmental water samples by utilizing

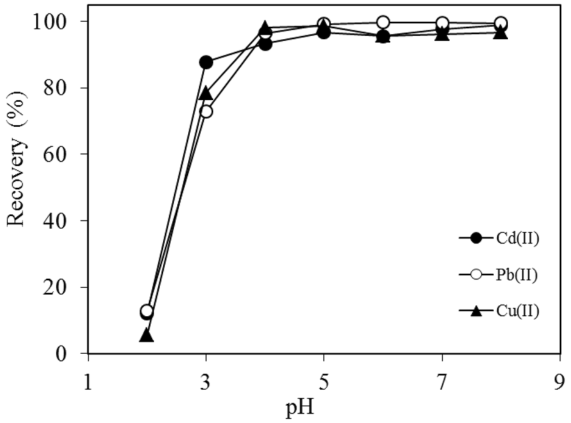

Fig. 6 Influence of pH on the analyte ions recovery (MPBC/$CoFe_2O_4$ amount 2.0 g L^{-1}, eluent type and volume 5.0 mL of 0.1 M HCl, adsorption and desorption contact time 5 min)

silica-coated magnetic graphene oxide nanocomposite as an adsorbent.

Evaluation of desorption solution type, concentration, and volume

In SPE procedures, the preference of an appropriate eluent plays a significant role to desorb the extracted analyte ions quantitatively. The complete and rapid desorption of the adsorbed analyte ions from the adsorbent surface is tremendously dependent on the type, concentration, and volume of the eluent used. The HNO_3 and HCl solutions are prevalently utilized as desorption solution without causing any interference effects in the analyses step and producing any hazardous wastes (Heidari et al., 2020). That is why, the influences of HNO_3 and HCl concentration on the recoveries of Cu^{2+}, Cd^{2+}, and Pb^{2+} ions were studied in the acid concentration range of 0.1–3.0 M under the optimum conditions. The quantitative recoveries were acquired when used 0.1 M HCl or 0.1 M HNO_3 solutions for all analyzed metal ions (Table 1). As the acid concentration increased from 0.5 to 3.0 M, the extraction efficiency of the analyte ions decreased considerably. This decrease may be due to as a result of decomposition of MPBC/$CoFe_2O_4$ at high acid concentrations (Khan et al., 2016). So, for further experiments, 0.1 M HCl was chosen as an effective, low cost, and eco-friendly elution solution to extract the analyte ions adsorbed by MPBC/$CoFe_2O_4$.

Table 1 Effect of eluent type and concentration on the extraction of the analyte ions (MPBC/$CoFe_2O_4$ amount 2.0 g L^{-1}, eluent volume 5.0 mL)

Eluent type	Recovery (%)		
	Pb(II)	Cd(II)	Cu(II)
0.1 M HCl	101.4 ± 1.5	99.4 ± 2.4	98.0 ± 0.9
0.5 M HCl	96.2 ± 1.7	95.6 ± 3.1	95.0 ± 0.3
1.0 M HCl	91.3 ± 1.9	91.1 ± 2.9	90.9 ± 1.8
2.0 M HCl	88.8 ± 4.8	88.3 ± 0.8	86.7 ± 3.4
3.0 M HCl	85.3 ± 1.0	83.3 ± 3.1	83.7 ± 2.8
0.1 M HNO_3	97.3 ± 1.2	98.9 ± 1.6	96.1 ± 3.1
0.5 M HNO_3	96.8 ± 2.6	93.3 ± 1.6	95.0 ± 0.3
1.0 M HNO_3	92.3 ± 1.9	90.6 ± 2.4	94.1 ± 1.5
2.0 M HNO_3	91.3 ± 4.1	89.4 ± 3.9	93.0 ± 2.5
3.0 M HNO_3	90.6 ± 3.8	87.2 ± 2.4	89.6 ± 1.7

In order to achieve high preconcentration factors, calculated by dividing the optimum sample volume by the eluent volume, it is necessary to choose the lowest volume of the eluent that provides quantitative recovery. Therefore the volume of 0.1 M HCl was assessed within the range of 2.5–10.0 mL. When the volume of HCl was increased from 2.5 to 5.0 mL, the extraction efficiencies increased from 74.4 to 96.8%, from 82.4 to 95.6%, and from 79.3 to 96.9% for Cu^{2+}, Cd^{2+}, and Pb^{2+} ions, respectively. In the HCl volume ranges of 5.0–10.0 mL, quantitative recovery values were obtained for all analyte ions. Consequently, the volume of 0.1 M HCl was optimized as 5.0 mL for the simultaneous determination of target ions throughout the SPE experiments.

Effect of MPBC/$CoFe_2O_4$ quantity

The influence of MPBC/$CoFe_2O_4$ dosage on the analyte ions recovery was assessed in the sorbent amount range of 1.0–15.0 g L^{-1}. As the MPBC/$CoFe_2O_4$ dosage was increased from 1.0 to 5.0 g L^{-1}, the recoveries of Cu^{2+}, Cd^{2+}, and Pb^{2+} ions increased from 94.9, 93.5, and 97.3 to 98.6%, 96.7%, and 97.5%, respectively, as a result of increase in the surface area and the binding sites for the adsorption of metal ions (Ghorbani et al., 2020). Although there was no considerable decrease for Cd^{2+} ions at MPBC/$CoFe_2O_4$ amounts

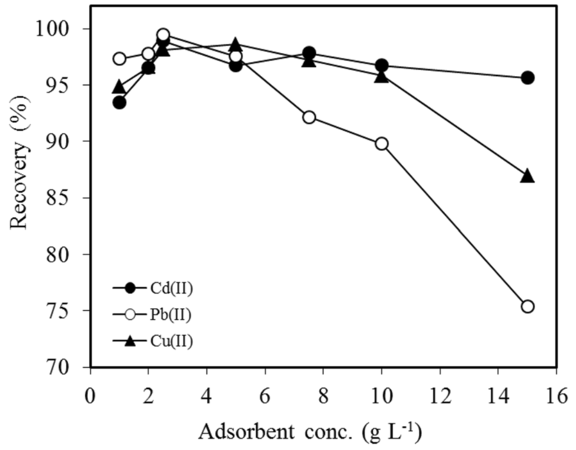

Fig. 7 Effect of MPBC/$CoFe_2O_4$ dosage on the extraction of analyte ions (pH 5.0, eluent type and volume 5.0 mL of 0.1 M HCl, adsorption and desorption contact time 5 min)

higher than 5.0 g L^{-1}, the recovery values for Cu^{2+} and Pb^{2+} ions decreased dramatically at higher adsorbent amounts. That is, the extraction efficiencies obtained for Cu^{2+}, Cd^{2+}, and Pb^{2+} ions at 15.0 g L^{-1} of MPBC/$CoFe_2O_4$ amount were 87.0%, 95.7%, and 75.4%, respectively (Fig. 7). This result may be due to the decrease in the strength of the eluent (5 mL of 0.1 M HCl) at high MPBC/$CoFe_2O_4$ amounts. Similar results were obtained by Assi et al. (2019) for the SPE of Cr^{6+} and Cr^{3+} ions using magnetic nanoparticles modified by 1,5-diphenylcarbazide. Accordingly, 2.0 g L^{-1} of MPBC/$CoFe_2O_4$ amount was chosen for further works.

Effect of sample volume

In order to determine the analyte ions accurately and sensitively in real samples, it is required to determine the optimum sample volume to which the method can be applied. The higher optimum sample volume contributes to achieve high preconcentration factors, thus enabling the detection of analyte ions present at very low levels in environmental samples. In this regard, the influence of sample volume was evaluated in the volume range of 50–1000 mL containing 20 µg of Pb^{2+}, 5 µg of Cd^{2+}, and 10 µg of Cu^{2+} ions and 2.0 g L^{-1} of MPBC/$CoFe_2O_4$ suspension at pH 5.0. The equilibrium time was kept as 5 min for each sample volume. The best extraction efficiencies were achieved by maximum applicable sample volume of 250 mL which are 97.6%, 95.6%, and 96.0% for Cu^{2+}, Cd^{2+}, and Pb^{2+} ions, respectively. The recovery values decreased distinctly while increasing the sample volume from 250 to 1000 mL. Thus, 250 mL was

Table 2 Influences of various foreign ions on the recovery of analyte ions (pH 5.0, sample volume 50 mL, MPBC/$CoFe_2O_4$ amount 2.0 g L^{-1}, eluent type and volume 5.0 mL of 0.1 M HCl, adsorption and desorption contact time 5 min)

Ions	Added as	Conc.(mg L^{-1})	Recovery (%)		
			Pb(II)	Cd(II)	Cu(II)
Na^+	NaCl	5000	93.4 ± 2.3	97.7 ± 3.4	97.4 ± 3.1
K^+	KCl	1000	96.3 ± 3.8	95.5 ± 3.9	92.9 ± 2.6
Ca^{2+}	$CaCl_2$	1000	101.2 ± 3.1	94.9 ± 2.9	97.6 ± 2.4
Mg^{2+}	$Mg(NO_3)_2$	1000	98.9 ± 1.3	97.2 ± 4.0	93.1 ± 1.7
CO_3^{2-}	Na_2CO_3	1000	99.7 ± 2.8	100.0 ± 1.6	96.7 ± 2.7
NO_3^-	$NaNO_3$	1000	99.6 ± 1.0	100.6 ± 2.4	95.5 ± 1.8
PO_4^{3-}	Na_3PO_4	1000	99.1 ± 0.8	92.6 ± 4.0	92.1 ± 1.7
NH_4^+	NH_4NO_3	1000	95.3 ± 1.6	92.0 ± 1.6	91.2 ± 2.4
Au(III), Mn(II), Cr(III), Zn(II)	*	25	97.4 ± 0.8	98.3 ± 0.8	97.5 ± 1.0
Mixed[a]			98.7 ± 1.6	91.5 ± 4.0	97.3 ± 2.6

*Their nitrate salts were used

[a] 687 mg L^{-1} Na^+, 1040 mg L^{-1} Cl^-, 960 mg L^{-1} NO_3^-, 100 mg L^{-1} K^+, Ca^{2+}, Mg^{2+}, CO_3^{2-}, PO_4^{3-}, NH_4^+, 10 mg L^{-1} Au(III), Mn(II), Cr(III), Zn(II)

Table 3 Isotherm constants for the metal ion adsorption onto MPBC/$CoFe_2O_4$

		Metal ions		
		Pb(II)	Cd(II)	Cu(II)
Langmuir isotherm model	Meaning of the constants			
q_{max} (mg g^{-1})	Adsorption amount per unit mass of MPBC/$CoFe_2O_4$ at equilibrium	188.7	65.4	106.4
b (L mg^{-1})	Adsorption energy	0.037	0.103	0.018
R^2		0.977	0.999	0.986
Freundlich isotherm model				
K_f (mg g^{-1})	Factor effecting the adsorption capacity	34.8	16.6	9.08
n	Adsorption intensity	3.86	4.32	2.58
R^2		0.476	0.889	0.981
D-R isotherm model				
q_m (mg g^{-1})	Monolayer adsorption capacity	15.7	10.4	13.4
β (kJ^2 mol^{-2})	Activity coefficient	−0.0021	−0.0025	−0.0044
E (kJ mol^{-1})	Mean adsorption energy	15.43	14.14	10.66
R^2		0.434	0.935	0.987

determined as optimum sample volume for the simultaneous determination of the analyte ions and the preconcentration factor was calculated as 50 when used 5.0 mL of eluent volume.

Effect of contact time for adsorption and desorption

In order to decide the adequate equilibrium time for the retention of Cu^{2+}, Cd^{2+}, and Pb^{2+} ions onto MPBC/$CoFe_2O_4$, the studies were performed in the equilibrium time range of 1–120 min by contacting 20.0 mg L^{-1} of Pb^{2+}, 2.0 mg L^{-1} of Cd^{2+}, and 5.0 mg L^{-1} of Cu^{2+} ions with 2.0 g L^{-1} of MPBC/$CoFe_2O_4$ suspensions at pH 5.0. When the solutions were shaken for 5 min, the q_e (mg g^{-1}) values of all analyte ions achieved their maximum values. Due to the rapid saturation of the active adsorption sites on the MPBC/$CoFe_2O_4$ surface, which were available substantially at the initial stages of the process, no significant change in the adsorption efficiency occurred after more than 5 min of agitation. As a consequence, a short contact time of 5 min was selected for complete adsorption of analyte ions on the MPBC/$CoFe_2O_4$.

The sufficient time for elution of Cu^{2+}, Cd^{2+}, and Pb^{2+} ions from MPBC/$CoFe_2O_4$ was assessed by changing the time in the range of 1–120 min. In these experiments, 2.0 g L^{-1} of MPBC/$CoFe_2O_4$ was mixed with 0.4 mg L^{-1} of Pb^{2+}, 0.1 mg L^{-1} of Cd^{2+}, and 0.2 mg L^{-1} of Cu^{2+} ions at pH 5.0. The volume of aqueous solution volume was 50 mL. At the end of the 5 min of adsorption time, the MPBC/$CoFe_2O_4$ was separated from the solution and treated with 5.0 mL of 0.1 M HCl solution in the time range of 1–120 min. The metal ions levels in the eluents were measured after being separated the adsorbent from the mixture at the end of each specified time period. The recovery values were 96.4%, 98.1%, and 96.1% for Cu^{2+}, Cd^{2+}, and Pb^{2+} ions, respectively, at the desorption contact time of 1 min. Hence, 1 min was designated as the optimum desorption time for the analyte ions. However, to make sure whether the adequate elution was obtained, the desorption contact time was specified as 5 min for subsequent studies. The short adsorption and desorption time is considered to be one of the most important advantages of the presented study. Zhu et al. (2016) have optimized the shaking time as 30 min for the SPE of Cr^{3+}, Fe^{3+}, Pb^{2+}, and Mn^{2+} ions from wastewater using carbon nanotubes functionalized with diethylenetriamine. Sun et al. (2015) have determined both the adsorption and desorption contact time as 7 min for magnetic SPE of different heavy metal ions from biological samples by utilizing magnetic graphene oxide nanocomposite.

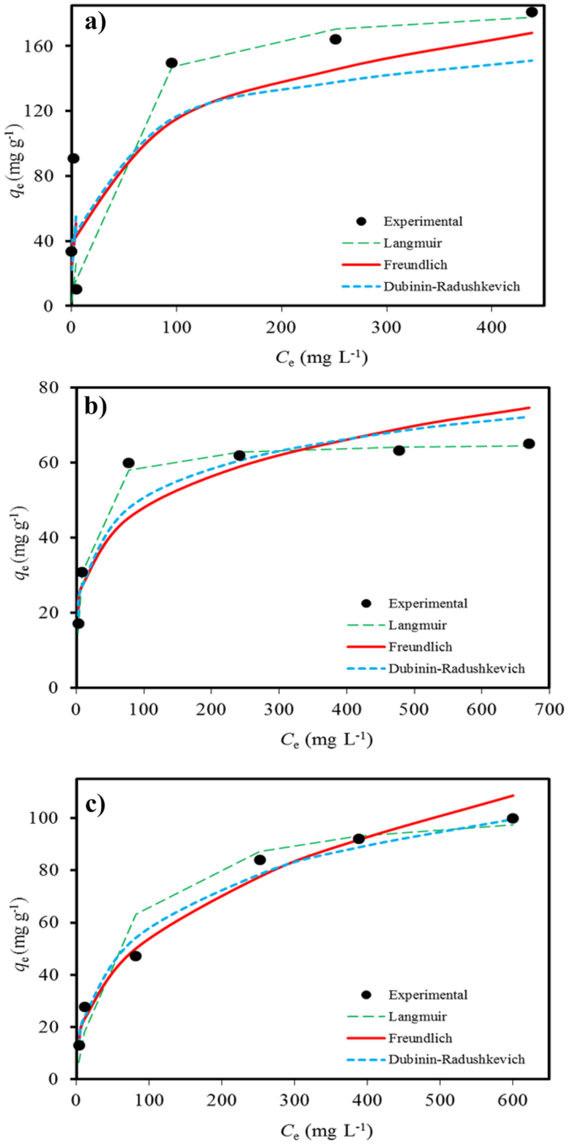

Fig. 8 Isotherms for the adsorption of metal ions onto MPBC/$CoFe_2O_4$

Effect of foreign ions

Most of the foreign ions present in the sample matrix may interfere the extraction efficiencies of the analyte ions. Therefore, to assess the performance and practicability of the method, the effects of potentially interfering ions generally found in environmental samples were evaluated by adding these ions at known concentrations to the 50 mL of model solutions containing 0.4 mg L^{-1} of Pb^{2+}, 0.1 mg L^{-1} of Cd^{2+}, and 0.2 mg L^{-1} of Cu^{2+} ions and 2.0 g L^{-1} of MPBC/$CoFe_2O_4$ suspension at pH 5.0. The solutions were treated according to the optimized SPE procedure. The obtained results revealed that the presence of most of the foreign ions at high levels have no notable effect on the simultaneous extraction and determination of target analyte ions indicating that the proposed method can be applied to the complicated matrices with high selectivity (Table 2).

Adsorption isotherms

In order to estimate the adsorption capacity of MPBC/$CoFe_2O_4$ and to interpret the adsorption mechanism of the analyte ions in more detailed, the Langmuir, Freundlich, and Dubinin-Radushkevich (D-R) isotherm models were implemented to the experimental data. For that purpose, the experiments were performed by using different initial metal ion concentrations (50–800 mg L^{-1}) at pH 5.0 by using 2.0 g L^{-1} of MPBC/$CoFe_2O_4$ amount. According to the graph plotted by the q_e values versus initial metal ion concentration (figure not shown), it was observed that the adsorption amount (q_e) increased from 10.4 to 180.0 mg g^{-1} for Pb^{2+}, from 17.2 to 65.0 mg g^{-1} for Cd^{2+}, and from 13.1 to 100.0 mg g^{-1} for Cu^{2+} ions as increasing the initial metal ion concentration from 50 to 800 mg L^{-1}.

Langmuir model supports the idea that the adsorption eventuates as a monolayer on the adsorbent surface, which is homogeneous and has active adsorption sites with equal energy (Langmuir, 1918). Conversely, Freundlich model is associated with the multilayer adsorption on heterogeneous adsorbent surface (Freundlich, 1906). The linear forms of Langmuir and Freundlich models are given in Eqs. 1 and 2, respectively.

$$\frac{C_e}{q_e} = \frac{C_e}{q_{max}} + \frac{1}{bq_{max}} \tag{1}$$

$$1\text{n}q_e = 1\text{n}K_f + \frac{1}{n}1\text{n}C_e \tag{2}$$

Table 4 Comparison of the method with recent studies on solid-phase extraction

SPE Adsorbent	Detection technique	Analyte	PF	LOD (μg L^{-1})	RSD (%)	Ads. capacity (mg g^{-1})	Ref
Fe_3O_4@SiO_2@ polyaminoquinoline nanocomposite	FAAS	Pb	207	0.7	6.5	73	Manoochehria et al. (2015)
		Cd		0.1	7.6	57	
Multiwalled carbon nanotubes/ cresolphthalein complexone	FAAS	Pb	40	3.52	-	-	Duran et al. (2009a)
		Cu		1.64			
Silica gel	FAAS	Pb	-	0.60	1.7	27.1	Xu et al. (2013)
		Cd		4.25	3.2	45.5	
CS/MOF-SH*	GF-AAS	Pb	25	0.033	3.9	425.3	Huang et al. (2020)
		Cd		0.008	4.1	109.9	
Magnetic allylamine modified graphene oxide-poly (vinylacetate-co-divinylbenzene)	FAAS	Pb	40	2.39	0.81	-	Khan et al. (2016)
		Cd		0.37	3.1		
		Cu		2.34	1.7		
EGBMA-MSPT-MNP**	ICP-OES	Pb	236	0.08	4.0	35.1	Mashhadizadeh et al. (2014)
		Cd	294	0.06	2.8	33.4	
		Cu	297	0.09	3.2	37.9	
Magnetic graphene oxide	FAAS	Pb	10	28.0	<2.1	9.9	Soylak et al. (2019)
		Cd		2.3		3.5	
		Cu		6.0		5.5	
Bismuthiol-II-immobilized magnetic nanoparticles	ICP-OES	Pb	87	0.085	3.7	9.4	Suleiman et al. (2009)
		Cu	95	0.058	4.6	5.3	
MWCNTs impregnated with D2EHPA-TOPO***	FAAS	Cu	25	50.0	<10	4.9	Vellaichamy and Palanivelu (2011)
Melon peel biochar/$CoFe_2O_4$	FAAS	Pb	50	3.16	3.10	188.7	This work
		Cd		1.82	4.19	65.4	
		Cu		0.41	2.34	106.4	

PF preconcentration factor, *LOD* limit of detection, *RSD* relative standard deviation

*Chitosan/thiol modified metal–organic frameworks

**Fe_3O_4 coated with 3-(trimethoxysilyl)-1-propanethiol and modified with ethylene glycol bis-mercaptoacetate

***Multiwalled carbon nanotubes impregnated with di-(2-ethyl hexyl phosphoric acid) and tri-n-octyl phosphine oxide

q_e (mg g^{-1}) and C_e (mg L^{-1}) are the adsorption amount per unit mass of MPBC/$CoFe_2O_4$ and the equilibrium concentration of metal ions, respectively.

The substantial feature of Langmuir model can be specified by R_L given by the following equation:

$$R_L = \frac{1}{1 + b.Co} \tag{3}$$

C_o (mg L^{-1}) describes the initial metal ion levels. For the acceptable process, R_L should be in the range of 0–1 (McKay et al., 1987).

D-R model is utilized to assess the metal ions adsorption mechanism (Dubinin & Radushkevich, 1947). The linear form of the model can be expressed as follows:

$$\text{In}\, q_e = \text{In}\, q_m - \beta\varepsilon^2 \tag{4}$$

ε is the Polanyi potential and calculated by Eq. 5:

$$\varepsilon = RTln(1 + 1/C_e) \tag{5}$$

R (8.314 J mol^{-1} K^{-1}) is the gas constant, T (K) is the temperature, and C_e (mol L^{-1}) is the metal ion levels in aqueous solution at equilibrium. The value of E is observed using Eq. 6:

$$E = 1/(-2\beta)^{1/2} \tag{6}$$

If the calculated E values are in the range of 8–16 kJ mol^{-1}, the adsorption process occurs through ion exchange. The physical and chemical adsorption mechanism is considered dominant when E values are lesser than 8 kJ mol^{-1} and higher than 16 kJ mol^{-1}, respectively (Mosai et al., 2020).

The Langmuir, Freundlich, and D-R isotherm constants were obtained from the linear plot of C_e/q_e versus C_e, lnq_e versus lnC_e, and In q_e versus ε^2, respectively, according to Eqs. 1, 2, and 4. The isotherm constants and correlation coefficients (R^2) are given in Table 3. The Langmuir, Freundlich, D-R isotherms, and experimental data are shown in Fig. 8. When the Langmuir and Freundlich models were compared, it can be said that the metal ion adsorption on the homogeneous MPBC/$CoFe_2O_4$ surface as a monolayer, since the R^2 for all three metal ion adsorption are higher for the Langmuir model. In addition, since the R^2 observed from the Freundlich model in the adsorption of Cu^{2+} ions is relatively high, it can be considered that the Cu^{2+} adsorption is also multilayered. The adsorption capacity of MPBC/$CoFe_2O_4$ was obtained as 188.7, 65.4, and 106.4 mg g^{-1} for Pb^{2+}, Cd^{2+}, and Cu^{2+} ions, respectively, by using Langmuir equation. The adsorption capacity of the proposed adsorbent is higher than most of the other reported sorbents given in Table 4 (Duran et al., 2009a; Huang et al., 2020; Khan et al., 2016; Manoochehria et al., 2015; Mashhadizadeh et al., 2014; Soylak et al., 2019; Suleiman et al., 2009; Vellaichamy & Palanivelu, 2011; Xu et al., 2013). Between 50 and 800 mg L^{-1} of initial metal ion concentrations, the R_L values were in the range of 0.35–0.03 for Pb^{2+}, 0.16–0.01 for Cd^{2+}, and 0.53–0.06 for Cu^{2+} ions which demonstrated the favorability of the process. The n values obtained from the Freundlich model were in the range of 1–10 also supported the suitability of the adsorption of Pb^{2+}, Cd^{2+}, and Cu^{2+} ions onto MPBC/$CoFe_2O_4$ (Le et al., 2019). The calculated E values using D-R model for all three metal ions were in the range of 8–16 kJ mol^{-1},

Table 5 Kinetics parameters for the metal ion adsorption onto MPBC/$CoFe_2O_4$

Metal ions	$q_{e\,exp}$ (mg g^{-1})	Pseudo-first order model			Pseudo-second order model			Intraparticle diffusion model				
		k_1 (min^{-1})	$q_{e\,cal}$ (mg g^{-1})	R^2	k_2 (g mg^{-1} min^{-1})	$q_{e\,cal}$ (mg g^{-1})	R^2	$k_{id,1}$ (mg g^{-1} min$^{-1/2}$)	R^2	$k_{id,2}$ (mg g^{-1} min$^{-1/2}$)	R^2	C
Pb(II)	9.80	-0.072	0.038	0.903	8.69	9.79	0.999	0.014	0.875	0.0009	0.660	9.76
Cd(II)	0.98	-0.087	0.103	0.931	3.62	0.99	0.999	0.051	0.819	0.0024	0.960	0.88
Cu(II)	2.49	-0.023	0.002	0.781	80.6	2.49	0.999	0.0003	0.994	0.0001	0.830	2.49

Table 6 Spike/recovery results of water samples (pH 5.0, sample volume 50 mL, eluent type and volume 5.0 mL of 0.1 M HCl)

Element	Added (μg)	Stream water		Sea water	
		Found (μg)	Recovery (%)	Found (μg)	Recovery (%)
Pb(II)	0	ND*	-	ND	-
	45	42.9 ± 1.1	95.3	44.3 ± 2.1	98.4
	90	84.8 ± 2.3	94.2	85.3 ± 3.0	94.8
Cd(II)	0	ND	-	ND	-
	5	4.87 ± 0.14	97.4	4.81 ± 0.18	96.2
	10	9.51 ± 0.25	95.1	9.56 ± 0.25	95.6
Cu(II)	0	ND	-	ND	-
	20	19.5 ± 0.4	97.5	19.1 ± 0.4	95.5
	40	38.1 ± 0.9	95.2	37.7 ± 0.5	94.3

*Not detected

indicating that the mechanisms of the adsorption of Cu^{2+}, Cd^{2+}, and Pb^{2+} ions onto MPBC/$CoFe_2O_4$ possibly take place via ion exchange mechanisms (Thamilarasi et al., 2018).

Adsorption kinetics

Adsorption kinetics was assessed by considering the pseudo-first-order (Lagergren, 1898) and pseudo-second-order kinetic models (Ho & McKay, 1998) and intraparticle diffusion models (Weber & Morriss, 1963) expressed by Eqs. 7, 8, and 9, respectively.

$$1\mathrm{n}\left(q_e - q_t\right) = 1\mathrm{n}q_e - k_1 t \tag{7}$$

$$\frac{t}{q_t} = \frac{1}{k_2 {q_e}^2} + \frac{t}{q_e} \tag{8}$$

$$q_t = k_{id} t^{1/2} + c \tag{9}$$

q_e (mg g^{-1}) indicates analyte ion levels adsorbed onto per unit mass of MPBC/$CoFe_2O_4$ at equilibrium; q_t (mg g^{-1}) denotes the amounts of the analyte ions adsorbed on the MPBC/$CoFe_2O_4$ at any time t; k_1 (min^{-1}), k_2 (g mg^{-1} min^{-1}), and k_{id} (mg g^{-1} $min^{-1/2}$); rate constants of first-order kinetics model, second-order kinetics model, and intraparticle diffusion models, respectively, C (mg g^{-1}); and intraparticle diffusion model constant (Gundogdu et al., 2012).

The pseudo-first order (PFO) and pseudo-second order (PSO) kinetic model parameters were observed from the intercept and slope of the linear plots of ln(q_e–q_t) versus t and t/q_t versus t, respectively, and given in Table 5. The R^2 values belonging to the PFO model were obtained as 0.781, 0.931 and 0.903 for Cu^{2+}, Cd^{2+}, and Pb^{2+} ions, respectively, while for PSO kinetic model, R^2 values were 0.999 for all three metal ions. Compared to the PFO, the adsorption mechanism of the analyte ions on MPBC/$CoFe_2O_4$ appears to be better assorted with the PSO kinetic model due to the high correlation coefficient and the proximity of q_e values obtained from the model to the experimental q_e values. This result demonstrated that the chemisorption mechanism is also possible in the process. Similar observations were reported by Buema et al. (2021) for the SPE of Cd^{2+} ions using hybrid inorganic $CoFe_2O_4$/carboxymethyl cellulose polymeric framework nanobeads. On the other hand, the intraparticle diffusion model was examined to explain the adsorption mechanism in more detail. By evaluating the q_t versus $t^{1/2}$ plots, it is seen that the adsorption process consists of three stages: film diffusion, intraparticle diffusion, and equilibrium state. Since the last step occurs very quickly, it is not effective in the adsorption mechanism. Whichever of the film diffusion or intraparticle diffusion steps has the smaller rate constant, that stage is considered to be more effective. As the rate constant values for both stages were compared, it is seen that the rate constants of the second stage have smaller values for all three metal ions; therefore, the intraparticle diffusion mechanism is considered to be effective in the metal ions adsorption onto MPBC/$CoFe_2O_4$. However, this assumption is valid when the line passes through its

Table 7 Spike/recovery results of solid samples (pH 5.0, sample volume 50 mL, sample quantities 0.750 g)

Element	Added (µg)	Pepper		Black cabbage		Eggplant		Tomato	
		Found (µg)	Recovery (%)	Found (µg)	Recovery (%)	Found (µg)	Recovery (%)	Found (µg)	Recovery (%)
Pb(II)	0	1.67 ± 0.04	-	5.09 ± 0.12	-	3.92 ± 0.13	-	3.89 ± 0.11	-
	45	45.3 ± 1.4	97.0	50.8 ± 1.7	101.6	47.8 ± 1.2	97.5	48.6 ± 1.9	99.4
	90	90.4 ± 2.3	98.6	94.5 ± 2.9	99.3	93.2 ± 2.8	99.2	92.2 ± 3.1	98.1
Cd(II)	0	ND	-	0.65 ± 0.01	-	0.75 ± 0.01	-	ND	-
	5	4.95 ± 0.18	99.0	5.40 ± 0.07	95.0	5.70 ± 0.11	99.0	5.04 ± 0.04	100.8
	10	9.93 ± 0.31	99.3	10.5 ± 0.3	98.5	11.2 ± 0.3	104.5	9.95 ± 0.20	99.5
Cu(II)	0	1.76 ± 0.03	-	2.48 ± 0.07	-	3.94 ± 0.04	-	2.81 ± 0.04	-
	10	12.2 ± 0.4	104.4	12.1 ± 0.2	96.2	13.3 ± 0.2	93.6	12.5 ± 0.3	96.9
	20	21.3 ± 0.5	97.7	21.9 ± 0.4	97.1	23.6 ± 0.5	98.3	21.7 ± 0.4	94.5

*Not detected

origin so that the *C* values are zero (Ozdes & Duran, 2014). The *C* constants were reported as 2.49, 0.88, and 9.76 for Cu^{2+}, Cd^{2+}, and Pb^{2+} ions, respectively, and hence, both film diffusion and intraparticle diffusion are considered to be impressive in the adsorption of Cu^{2+}, Cd^{2+}, and Pb^{2+} ions onto MPBC/$CoFe_2O_4$ (Ozdes et al., 2014).

Analytical performance of the method

To determine the limit of detection (LOD), the optimized method was applied to ten blank solutions. The LODs were calculated by taking three times the standard deviations of the analysis results of the blank solutions and obtained as 0.41, 1.82, and 3.16 µg L^{-1} for Cu^{2+}, Cd^{2+}, and Pb^{2+} ions, respectively. The relative standard deviation (RSD) that gives idea about the precision of the method was calculated by applying the optimized procedure ten times using 50 mL of aqueous solutions containing 0.4 mg L^{-1} of Pb^{2+}, 0.1 mg L^{-1} of Cd^{2+}, and 0.2 mg L^{-1} of Cu^{2+} ions. Based on the results, the RSDs were 2.34, 4.19 and 3.10% for Cu^{2+}, Cd^{2+}, and Pb^{2+} ions, respectively. The figures of merits of the proposed method were compared with those of other reported SPE procedures, as summarized in Table 4. It is evident that the MPBC/$CoFe_2O_4$-based SPE method has lower RSD and LOD and also higher preconcentration factor when compared to most of the previous methods.

Method accuracy and application to real samples

The aim of optimizing the experimental parameters in detail is to offer a method for simultaneous detection of Cu^{2+}, Cd^{2+}, and Pb^{2+} ions in environmental liquid and solid samples. On the other hand, the accuracy and applicability of the optimized method were estimated by spiking different amounts of analyte ions to sea and stream waters (Table 6) and to pepper, black cabbage, eggplant, and tomato samples (Table 7). Sufficient conformity was observed between the added and found analyte levels, demonstrating the validity of the suggested method. As a conclusion, the proposed method was applied successfully to determine the heavy metal levels of water and vegetable samples (Table 8).

Table 8 Application to real samples (pepper, black cabbage, eggplant, tomato amount 0.750 g, sea and stream water volume 250 mL, final volume 5.0 mL)

Element	Liquid samples (μg L^{-1})		Solid samples (μg g^{-1})			
	Sea water	Stream water	Pepper	Black cabbage	Eggplant	Tomato
Pb(II)	3.43 ± 0.16	7.50 ± 0.99	2.23 ± 0.07	6.79 ± 0.25	5.23 ± 0.18	5.19 ± 0.21
Cd(II)	ND*	ND	ND	0.87 ± 0.01	1.00 ± 0.03	ND
Cu(II)	20.4 ± 1.1	8.15 ± 0.66	2.35 ± 0.06	3.31 ± 0.05	5.25 ± 0.14	3.75 ± 0.05

*Not detected

Conclusions

In this paper, a simple, effective, and environmentally friendly magnetic solid-phase extraction technique using melon peel biochar modified with $CoFe_2O_4$ as a new adsorbent was developed. The experimental parameters were optimized, and the method validation was performed by the spike/recovery tests. Thereafter, the MPBC/$CoFe_2O_4$ was successfully utilized for separation, preconcentration, and simultaneous determination of Cu^{2+}, Cd^{2+}, and Pb^{2+} ions in waters and some vegetable samples without significant matrix interferences. There is no need to use any special laboratory equipment in the process. This demonstrated the cheapness of the method. The quantitative recovery values were obtained in a wide pH range (4.0–8.0). The low adsorption and desorption contact time, low LOD and RSD values, and the obtained high metal adsorption capacity of MPBC/$CoFe_2O_4$ are considered as crucial advantages of the suggested method. As a result, it is considered that this study provide a new and beneficial approach for the assessment of trace heavy metal ions in waters and vegetable samples.

Funding The financial support was received from the Unit of the Scientific Research Projects of Karadeniz Technical University.

Availability of data and material All data generated or analyzed during this study are included in this published article.

Code availability Not applicable.

Declarations

Ethics approval Not applicable.

Consent to participate Not applicable.

Consent for publication Not applicable.

Competing interests The authors declare no competing interests.

References

Ahmadi, M., Kouhgardi, E., & Ramavandi, B. (2016). Physicochemical study of dew melon peel biochar for chromium attenuation from simulated and actual wastewaters. *Korean Journal of Chemical Engineering, 33*(9), 2589–2601.

Amin, M. T., Alazba, A. A., & Shafiq, M. (2019). Comparative study for adsorption of methylene blue dye on biochar derived from orange peel and banana biomass in aqueous solutions. *Environmental Monitoring and Assessment, 191*, 735.

Assi, N., Azar, P. A., Tehrani, M. S., Husain, S. W., Darwish, M., & Pourmand, S. (2019). Selective solid phase extraction using 1,5-diphenylcarbazide-modified magnetic nanoparticles for speciation of Cr(VI) and Cr(III) in aqueous solutions. *International Journal of Environmental Science and Technology, 16*, 4739–4748.

Behbahani, M., Salarian, M., Amini, M. M., Sadeghi, O., Bagheri, A., & Bagheri, S. (2013). Application of a new functionalized nanoporous silica for simultaneous trace separation and determination of Cd(II), Cu(II), Ni(II), and Pb(II) in food and agricultural products. *Food Analytical Methods, 6*, 1320–1329.

Bigdeli, M., & Seilsepour, M. (2008). Investigation of metals accumulation in some vegetables irrigated with waste water in Shahre Rey-Iran and toxicological implications. *American-Eurasian Journal of Agricultural & Environmental Sciences, 4*, 86–92.

Buema, G., Borhan, A. I., Herea, D. D., Stoian, G., Chiriac, H., Lupu, N., Roman, T., Pui, A., Harja, M., & Gherca, D. (2021). Magnetic solid-phase extraction of cadmium ions by hybrid self-assembled multicore type nanobeads. *Polymers, 13*, 229.

Dahaghin, Z., Mousavi, H. Z., & Sajjadi, S. M. (2017). Trace amounts of Cd(II), Cu(II) and Pb(II) ions monitoring using Fe_3O_4@graphene oxide nanocomposite modified via 2-mercaptobenzothiazole as a novel and efficient nanosorbent. *Journal of Molecular Liquids, 231*, 386–395.

Dubinin, M. M., & Radushkevich, L. V. (1947). Equation of the characteristic curve of activated charcoal. *Proceedings of the Academy of Sciences of the USSR, Physical Chemistry Section, 55*, 331–333.

Duran, A., Tuzen, M., & Soylak, M. (2009a). Preconcentration of some trace elements via using multiwalled carbon nanotubes as solid phase extraction adsorbent. *Journal of Hazardous Materials, 169*, 466–471.

Duran, C., Bulut, V. N., Gundogdu, A., Ozdes, D., Yildirim, N., Soylak, M., Senturk, H. B., & Elci, L. (2009b). Carrier element-free coprecipitation with 3-phenly-4-o-hydroxybenzylidenamino-4,5-dihydro-1,2,4-triazole-5-one for separation/preconcentration of Cr(III), Fe(III), Pb(II) and Zn(II) from aqueous solutions. *Journal of Hazardous Materials, 167*(1–3), 294–299.

Farajvand, M., Kiarostami, V., Davallo, M., & Ghaedi, A. (2019). Simultaneous extraction of Cu^{2+} and Cd^{2+} ions in water, wastewater, and food samples using solvent-terminated dispersive liquid–liquid microextraction: Optimization by multiobjective evolutionary algorithm based on decomposition. *Environmental Monitoring and Assessment, 191*, 287.

Foroutan, R., Mohammadi, R., Ramavandi, B., & Bastanian, M. (2018). Removal characteristics of chromium by activated carbon/ $CoFe_2O_4$ magnetic composite and *Phoenix dactylifera* stone carbon. *Korean Journal of Chemical Engineering, 35*(11), 2207–2219.

Freundlich, H. M. F. (1906). Uber die adsorption in lösungen. *Zeitschrift Für Physikalische Chemie, 57*, 385–470.

Ghorbani, Y. A., Ghoreishi, S. M., & Ghani, M. (2020). Derived N-doped carbon through core-shell structured metal-organic frameworks as a novel sorbent for dispersive solid phase extraction of Cr(III) and Pb(II) from water samples followed by quantitation through flame atomic absorption spectrometry, *Microchemical Journal*, *155*, 104786.

Gouda, A. A. (2014). Solid-phase extraction using multiwalled carbon nanotubes and quinalizarin for preconcentration and determination of trace amounts of some heavy metals in food, water and environmental samples. *International Journal of Environmental Analytical Chemistry, 94*, 1210–1222.

Gundogdu, A., Duran, C., Senturk, H. B., Soylak, M., Ozdes, D., Serencam, H., & Imamoglu, M. (2012). Adsorption of phenol from aqueous solution on a low-cost activated carbon produced from tea ındustry waste: Equilibrium, kinetic, and thermodynamic study. *Journal of Chemical Engineering Data, 57*, 2733–2743.

Han, L., Nie, X., Wei, J., Gu, M., Wu, W., & Chen, M. (2021). Effects of feedstock biopolymer compositions on the physiochemical characteristics of dissolved black carbon from lignocellulose-based biochar. *Science of the Total Environment*, *751*, 141491.

Heidari, M., Ghanemi, K., & Nikpour, Y. (2020). Applying Al_2O_3@Ag@trithiocyanuric acid as an efficient metal ion scavenger for the selective extraction of iron (III) and lead (II) from environmental waters. *Ecotoxicology and Environmental Safety*, *203*, 110995.

Ho, Y. S., & McKay, G. (1998). Kinetic models for the sorption of dye from aqueous solution by wood. *Journal of Environment Science Health. Part B: Process Safety and Environmental Protection, 76,* 183–191.

Huang, L., Huang, W., Shen, R., & Shuai, Q. (2020). Chitosan/thiol functionalized metal–organic framework composite for the simultaneous determination of lead and cadmium ions in food samples. *Food Chemistry*, *330*, 127212.

Kanani, N., Bayat, M., Shemirani, F., Ghasemi, J. B., Bahrami, Z., & Badiei, A. (2018). Synthesis of magnetically modified mesoporous nanoparticles and their application in simultaneous determination of Pb(II), Cd(II) and Cu(II). *Research on Chemical Intermediates, 44*, 1689–1709.

Khan, M., Yilmaz, E., Sevinc, B., Sahmetlioglu, E., Shah, J., Jan, M. R., & Soylak, M. (2016). Preparation and characterization of magnetic allylamine modified graphene oxide-poly(vinylacetate-co-divinylbenzene) nanocomposite for vortex assisted magnetic solid phase extraction of some metal ions. *Talanta, 146*, 130–137.

Lagergren, S. (1898). About the theory of so-called adsorption of soluble substance. *Kung Sven. Veten. Hand., 24*, 1–39.

Langmuir, I. (1918). The adsorption of gases on plane surfaces of glass, mica and platinum. *Journal of the American Chemical Society, 40*, 1361–1403.

Le, V. T., Tran, T. K. N., Tran, D. L., Le, H. S., Doan, V. D., Bui, Q. D., & Nguyen, H. T. (2019). One-pot synthesis of a novel magnetic activated carbon/clay composite for removal of heavy metals from aqueous solution. *Journal of Dispersion Science and Technology, 40*(12), 1761–1776.

Li, X., Wang, C., Zhang, J., Liu, J., Liu, B., & Chen, G. (2020). Preparation and application of magnetic biochar in water treatment: A critical review. *Science of the Total Environment*, *711*, 134847.

Li, S., Wu, Y., Zheng, Y., Jing, T., Tian, J., Zheng, H., Wang, N., Nan, J., & Ma, J. (2021). Free-radical and surface electron transfer dominated bisphenol A degradation in system of ozone and peroxydisulfate co-activated by $CoFe_2O_4$-biochar. *Applied Surface Science, 541*, 147887.

Manoochehria, M., Asgharinezhad, A. A., & Shekari, N. (2015). Synthesis, characterisation and analytical application of Fe_3O_4@SiO_2@polyaminoquinoline magnetic nanocomposite for the extraction and preconcentration of Cd(II) and Pb(II) in food samples. *Food Additives & Contaminants: Part A, 32*, 737–747.

Mashhadizadeh, M. H., Amoli-Diva, M., Shapouri, M. R., & Afruzi, H. (2014). Solid phase extraction of trace amounts of silver, cadmium, copper, mercury, and lead in various food samples based on ethylene glycol bis-mercaptoacetate modified 3-(trimethoxysilyl)-1-propanethiol coated Fe_3O_4 nanoparticles. *Food Chemistry, 151*, 300–305.

McKay, G., El-Guendi, M., & Nassar, M. (1987). Equilibrium studies during the removal of dyestuffs from aqueous solutions using bagasse pith. *Water Research, 21*, 1513–1520.

Mehrabi, F., Vafaei, A., Ghaedi, M., Ghaedi, A. M., Dil, E., & Asfaram, A. A. (2017). Ultrasound assisted extraction of Maxilon Red GRL dye from water samples using cobalt ferrite nanoparticles loaded on activated carbon as sorbent: Optimization and modeling. *Ultrasonics Sonochemistry, 38*, 672–680.

Mosai, A. K., Chimuka, L., Cukrowska, E. M., Kotze, I. A., & Tutu, H. (2020). Removal of platinum (IV) from aqueous solutions with yeast functionalized bentonite. *Chemosphere*, *239*, 124768.

Ozdes, D., & Duran, C. (2014). Preparation of a new sorbent, cetyltrimethylammonium bromide (CTAB)- modified obsidian, for the separation and preconcentration of Pb(II) and Cd(II) ions in food and water samples. *Atomic Spectroscopy, 35*, 118–126.

Ozdes, D., Duran, C., Senturk, H. B., Avan, H., & Bicer, B. (2014). Kinetics, thermodynamics and equilibrium evaluation of adsorptive removal of methylene blue onto natural ıllitic clay mineral. *Desalination and Water Treatment, 52*, 208–218.

Rahimi, Z., Sarafraz, H., Alahyarizadeh, Gh., & Shirani, A. S. (2018). Hydrothermal synthesis of magnetic $CoFe_2O_4$ nanoparticles and $CoFe_2O_4$/MWCNTs nanocomposites for U and Pb removal from aqueous solutions. *Journal of Radioanalytical and Nuclear Chemistry, 317*, 431–442.

Rahnama, R., & Najafi, M. (2016). The use of rapidly synergistic cloud point extraction for the separation and preconcentration of trace amounts of Ni (II) ions from food and water samples coupling with flame atomic absorption spectrometry determination. *Environmental Monitoring and Assessment, 188*, 150.

Ramadan, R. (2019). Physical study of cobalt ferrite and its application in purification of water. *Applied Physics A, 125*, 825.

Reddy, D. H. K., & Lee, S.-M. (2014). Magnetic biochar composite: Facile synthesis, characterization, and application for heavy metal removal. *Colloids and Surfaces a: Physicochemical and Engineering Aspects, 454*, 96–103.

Soylak, M., Acar, D., Yilmaz, E., El-Khodary, S. A., Morsy, M., & Ibrahim, M. (2019). Magnetic graphene oxide as an efficient adsorbent for the separation and preconcentration of Cu(II), Pb(II), and Cd(II) from environmental samples. *Journal of AOAC International, 100*, 1544–1550.

Soylak, M., Narin, I., Divrikli, U., Saracoglu, S., Elci, L., & Dogan, M. (2004). Preconcentration-separation of heavy metal ions in environmental samples by membrane filtration-atomic absorption spectrometry combination. *Analytical Letters, 37*, 767–780.

Suleiman, J. S., Hu, B., Peng, H., & Huang, C. (2009). Separation/preconcentration of trace amounts of Cr, Cu and Pb in environmental samples by magnetic solid-phase extraction with Bismuthiol-II-immobilized magnetic nanoparticles and their determination by ICP-OES. *Talanta, 77*, 1579–1583.

Sun, J., Liang, Q., Han, Q., Zhang, X., & Ding, M. (2015). One-step synthesis of magnetic graphene oxide nanocomposite and its application in magnetic solid phase extraction of heavy metal ions from biological samples. *Talanta, 132*, 557–563.

Suo, L., Dong, X., Gao, X., Xu, J., Huang, Z., Ye, J., Lu, X., & Zhao, L. (2019). Silica-coated magnetic graphene oxide nanocomposite based magnetic solid phase extraction of trace amounts of heavy metals in water samples prior to determination by inductively coupled plasma mass spectrometry. *Microchemical Journal*, *149*, 104039.

Thamilarasi, M. J. V., Anilkumar, P., Theivarasu, C., & Sureshkumar, M. V. (2018). Removal of vanadium from wastewater using surface-modified lignocellulosic material. *Environmental Science and Pollution Research, 25*, 26182–26191.

Tokay, F., & Bagdat, S. (2019). Solid phase extraction and preconcentration of some metal ions using Schiff base immobilised silica gel followed by ICP-OES. *International Journal of Environmental Analytical Chemistry, 99*, 1528–1539.

Tu, Y., Ju, S., & Wang, P. (2016). Flame atomic absorption spectrometric determination of copper, lead, and cadmium in Gastrodiae rhizoma samples after preconcentration using magnetic solid-phase extraction. *Spectroscopy Letters, 49*, 249–256.

Tufekci, M., Bulut, V. N., Elvan, H., Ozdes, D., Soylak, M., & Duran, C. (2013). Determination of Pb(II), Zn(II), Cd(II) and Co(II) ions by flame atomic absorption spectrometry in food and water samples after preconcentration by coprecipitation with Mo(VI)-diethyldithiocarbamate. *Environmental Monitoring and Assessment, 185*, 1107–1115.

Vellaichamy, S., & Palanivelu, K. (2011). Preconcentration and separation of copper, nickel and zinc in aqueous samples by flame atomic absorption spectrometry after column solid-phase extraction onto MWCNTs impregnated with D2EHPA-TOPO mixture. *Journal of Hazardous Materials, 185*, 1131–1139.

Weber, W. J., Jr., & Morriss, J. C. (1963). Kinetics of adsorption on carbon from solution. *Journal of the Sanitary Engineering Division, American Society of Civil Engineers, 89*, 31–60.

Xu, H., Wu, Y., Wang, J., Shang, X., & Jiang, X. (2013). Simultaneous preconcentration of cadmium and lead in water samples with silica gel and determination by flame atomic absorption spectrometry. *Journal of Environmental Sciences, 25*, S45–S49.

Yağci, Ö., Akkaya, E., & Bakirdere, S. (2020). Nano-sized magnetic Ni particles based dispersive solid-phase extraction of trace Cd before the determination by flame atomic absorption spectrometry with slotted quartz tube: A new, accurate, and sensitive quantification method. *Environmental Monitoring and Assessment, 192*, 583.

You, Y., Shi, Z., Li, Y., Zhao, Z., He, B., & Cheng, X. (2021). Magnetic cobalt ferrite biochar composite as peroxymonosulfate activator for removal of lomefloxacin hydrochloride. *Separation and Purification Technology, 272*, 118889.

Zhang, S., Ji, Y., Dang, J., Zhao, J., & Chen, S. (2019). Magnetic apple pomace biochar: Simple preparation, characterization, and application for enriching Ag(I) in effluents. *Science of the Total Environment, 668*, 115–123.

Zhao, D., Li, J., Li, C., Juhasz, A. L., Scheckel, K. G., Luo, J., Li, H.-B., & Ma, L. Q. (2016). Lead relative bioavailability in lip products and their potential health risk to women. *Environmental Science and Technology, 50*(11), 6036–6043.

Zhao, J., Liang, G., Zhang, X., Cai, X., Li, R., Xie, X., & Wang, Z. (2019). Coating magnetic biochar with humic acid for high efficient removal of fluoroquinolone antibiotics in water. *Science of the Total Environment, 688*, 1205–1215.

Zhou, L., Ji, L., Ma, P.-C., Shao, Y., Zhang, H., Gao, W., & Li, Y. (2014). Development of carbon nanotubes/ $CoFe_2O_4$ magnetic hybrid material for removal of tetrabromobisphenol A and Pb(II). *Journal of Hazardous Materials, 265*, 104–114.

Zhu, X., Cui, Y., Chang, X., & Wang, H. (2016). Selective solid-phase extraction and analysis of trace-level Cr(III), Fe(III), Pb(II), and Mn(II) ions in waste water using diethylenetriamine-functionalized carbon nanotubes dispersed in graphene oxide colloids. *Talanta, 146*, 358–363.